scientific reports

Check for updates

OPEN

Rapamycin alleviates hypothalamic injury in exertional heat stroke rats by activating mitophagy through the mTOR/Pink1/Parkin pathway

Ruxue Chi[1,4], Yan Gu[3,4]✉, Ran Meng[1], Lv Xuan[2], Zhengzhong Sun[1], Yuxiang Zhang[3]✉ & Jiaxing Wang[3]✉

Exertional heat stroke (EHS) causes severe central nervous system damage, with mitochondrial dysfunction and oxidative stress playing major roles. Mitophagy, regulated by the Pink1/Parkin pathway, removes damaged mitochondria. Here, we investigated the potential of rapamycin (RAPA) to reduce hypothalamic injury in rats subjected to EHS. Forty healthy male Sprague–Dawley rats were randomly assigned to control, RAPA, EHS, and EHS + RAPA groups (10 rats each). Core temperatures were measured, and survival curves were generated. Hypothalamic tissue underwent hematoxylin-eosin and Nissl staining for histopathological assessment. Hypothalamic mitochondrial membrane potential, reactive oxygen species (ROS), and malonaldehyde (MDA) levels were measured. Western blotting assessed mammalian target of RAPA (mTOR), phosphorylated mTOR, Pink1, Parkin, P62, and microtubule-associated protein 1 Light chain 3 (LC3) expression, and calculated the LC3II/LC3I ratio. Immunofluorescence evaluated Pink1-Parkin and LC3-Tom20 co-localization in hypothalamic tissue. EHS and EHS + RAPA groups showed markedly increased core temperatures. RAPA mitigated pathological injury and apoptosis, reduced ROS and MDA levels, and enhanced mitochondrial membrane potential. It downregulated mTOR and p62 levels, upregulated Pink1 and Parkin, increased LC3II/LC3I ratio, and promoted LC3-Tom20 and Pink1-Parkin interactions in the hypothalamic tissue of rats treated with EHS, thereby alleviating hypothalamic injury and preserving hypothalamic function.

Keywords Heat stroke, Hypothalamus, Rapamycin, Mitophagy, Pink1, Parkin

Heat stroke (HS) is characterized by high fever and central nervous system damage, with symptoms including delirium, convulsions, and coma. HS is classified as a systemic inflammatory response syndrome that can lead to multiple organ dysfunction, including brain impairment. Without appropriate treatment, HS is associated with a high risk of disability and fatality. HS can be divided into two categories based on its cause: classic HS and exertional HS (EHS)[1].

The cerebral cortex, hippocampus, and hypothalamus are the areas of the central nervous system most susceptible to HS injury[2]. The paraventricular nucleus (PVN) directly regulates the hypothalamic–pituitary–adrenal axis. After heat shock, damage to the small cells and neurons in the PVN reduces the body's heat tolerance and impairs its thermoregulatory function, considerably worsening the prognosis[3].

Heat shock can directly damage mitochondria, generate large amounts of reactive oxygen species (ROS), increase intracellular oxidative stress, and trigger inflammation[4–6]. Additionally, oxidative stress and inflammation further damage mitochondria and erode telomeres[7], creating a vicious cycle that amplifies oxidative stress, eventually leading to systemic inflammatory response syndrome and organ failure. Therefore, effective and selective removal of damaged mitochondria is critical for minimizing organ damage caused by HS.

Mitochondrial autophagy is the process by which damaged, aging, and dysfunctional mitochondria are selectively recognized by autophagosomes and transported to lysosomes for degradation in a process that is essential for maintaining mitochondrial quality and dynamic balance[8]. The key regulatory pathways for

[1]Graduate School of Hebei North University, Zhangjiakou 075000, China. [2]The Fourth Affiliated Hospital of Harbin Medical University, Harbin 150001, China. [3]Department of Critical Care Medicine, the Eighth Medical Center of Chinese PLA General Hospital, Beijing 100091, China. [4]These authors contributed equally: Ruxue Chi and Yan Gu. ✉email: 1148422140@qq.com; 15810550308@163.com; togzy11@163.com

mitophagy involve PTEN-induced kinase 1 (Pink1) and RBR E3 ubiquitin-protein ligase (Parkin)[9]. It has been shown that mitophagy upregulation can reduce liver injury caused by heat radiation in rats[10]. However, research on the role of the Pink1/Parkin pathway in hypothalamic injury during HS remains limited.

Rapamycin (RAPA) specifically inhibits the activity of the mammalian target of RAPA (mTOR), enhances autophagy, and reduces neuronal damage[11]. Previous studies have demonstrated that the hypothalamic function was preserved by inhibiting the mTOR pathway and promoting autophagy[12]. Therefore, in this study, we established an EHS rat model to investigate whether RAPA can enhance mitophagy and reduce hypothalamic injury caused by EHS by activating the Pink1/Parkin pathway. Our findings provide a theoretical basis for the treatment of central nervous system dysfunction in patients with EHS.

Materials and methods

Animals, instruments, and reagents

Forty healthy male Sprague–Dawley rats (8 weeks old, weighing 300–500 g) were purchased from SPF Biotechnology Co., Ltd. (Beijing, China; License number: SCXK (Jing) 2019-0010). The rats were housed in an SPF-grade animal laboratory at the Eighth Medical Center of the Chinese PLA General Hospital, with adequate ventilation, a 12-h light/dark cycle, a temperature of 25–26 ℃, and relative humidity of 50–60%. The Animal Ethics Committee of the Eighth Medical Center of the PLA General Hospital approved all animal experiments. (approval number:309202011301010)

Six small animal treadmill stages (XR-PT-10 A; Shanghai Xinruan Information Technology Co., Ltd) were placed in a transparent, simulated high-temperature and high-humidity environment chamber, which accurately controlled and maintained a constant temperature and humidity. A rat rectal thermometer (TH212; Shanghai Yuyan Technology Instrument Co., Ltd), with a sensitivity of 0.1 ℃ and an accuracy of ≤ ± 0.2 ℃, was used. RAPA (25 mg) was purchased from MCE.

Rabbit anti-rat glyceraldehyde 3-phosphate dehydrogenase (GAPDH) monoclonal antibody and rabbit anti-rat microtubule-associated protein 1 Light chain 3 (LC3) polyclonal antibody were purchased from CST (USA). Rabbit anti-rat Pink1 polyclonal antibody, rabbit anti-rat Parkin polyclonal antibody, rabbit anti-rat monoclonal antibody p62, and rabbit anti-rat monoclonal antibody Tom20 were purchased from Abcam (UK). Rabbit anti-rat monoclonal antibodies to mTOR and phosphorylated mTOR (p-mTOR) were purchased from Proteintech (USA). Goat anti-rabbit polyclonal antibody conjugated with horseradish peroxidase was obtained from Beijing Zhongshan Jinqiao Biotechnology Co., Ltd. The TdT-mediated dUTP nick-end labeling (TUNEL) kit was purchased from Roche, Switzerland. IL-6 and TNF-α enzyme-linked immunosorbent assay (ELISA) kits were obtained from Abcam, UK. The ROS and malondialdehyde (MDA) detection kits were purchased from Wuhan Saipei Biotechnology Co., Ltd. A spot image acquisition and processing system (Nikon, Japan) and a gel imaging system (Bio-Rad, USA) were used. Mitochondrial Membrane Potential Assay Kit with JC-1 was purchased from Shanghai Juncheng Biotechnology Co, Ltd. All other reagents were domestic analytical pure.

Animal grouping and model construction

Forty healthy male Sprague–Dawley rats were randomly divided into four groups using the random number table method: control (CON group), RAPA (RAPA group), EHS (EHS group), and EHS + RAPA (EHS + RAPA group), with 10 rats per group. Before EHS modeling, the rats underwent adaptation training in a thermal environment chamber using a step training method at an indoor temperature of 24–26 ℃ for 7 days. RAPA was dissolved in 100% DMSO and prepared as a 2 g/L stock solution; 15 μL of this solution was mixed with Tween-80 and normal saline and diluted to a final volume of 1.5 mL as the working solution. Rats in the RAPA and EHS + RAPA groups were intraperitoneally injected with the working solution at a dose of 1 mg/kg/day at 0800 h for 7 consecutive days before modeling. Rats in the CON and EHS groups received an equivalent volume of normal saline in the same period.

Before the EHS experiment, the rats were fasted for 12 h with water available ad Libitum. Thirty minutes before modeling, the rats were weighed and were prevented from drinking water for 30 min to stimulate defecation. When the temperature of the experimental chamber reached 39.5 ± 0.3 ℃ and the relative humidity reached 55% ± 5%, the rats were placed on a treadmill and started running at an initial speed of 5 m/min (with no incline). The speed was increased by 1 m/min every 2 min until reaching 15 m/min after 20 min, after which the rats continued running at a constant speed until fatigue (defined as the inability to continue running)[13]. Consciousness and mental status were closely observed throughout the experiment[14]. Once the diagnostic criteria for EHS were met, the rats were removed from the hot chamber and heat exposure was stopped. The rats were weighed and allowed to cool naturally at room temperature (24–26 ℃), and their mental states were monitored until 5 h after modeling. The diagnostic criterion for EHS was central nervous system dysfunction, indicated by a lack of autonomous activity for more than 5 s, with mild stimulation unable to induce movement.

At the 5th hour after the establishment of EHS, the rats were sacrificed for the following experiments.

Core temperature monitoring in rats

During modeling, a Lubricated anal thermometer sensor was inserted 5–7 cm into the rat's rectum. The sensor was secured to the tail using medical tape to prevent displacement. The rat's core temperature Ranged between 37 and 38 ℃ before entering the chamber, and core temperature measurements were recorded every 10 min once they were inside. Changes in core temperature were observed in each group, and a dynamic core temperature curve was plotted.

Histopathological observation of the hypothalamus in rats

The right hypothalamic tissue was isolated, rinsed with phosphate-buffered saline (PBS), and fixed in 4% paraformaldehyde. After dehydration with a graded ethanol series, the tissue was embedded in paraffin,

sectioned at 5 μm, and stained with hematoxylin-eosin (HE) and Nissl stains following deparaffinization. Histopathological changes in the hypothalamus were then observed under a light microscope after dehydration. Ten visual fields were randomly selected using a DM4000B optical microscope, and hypothalamic injury was scored based on the neuronal injury scoring criteria established by Thoresen et al.[15].

Detection of mitochondrial membrane potential in hypothalamic tissue

Approximately 100 μg of fresh left hypothalamic tissue was collected, and 10 volumes of mitochondrial separation reagent were added. The tissue was homogenized using a glass homogenizer and then centrifuged to obtain the supernatant. The mitochondria were extracted and purified by differential centrifugation. The prepared JC-1 staining working solution was diluted 5 times with JC-1 staining buffer (1×). 0.9 mL of the 5-fold diluted JC-1 staining working solution was added to 0.1 mL of purified mitochondria with a total protein content of 100 μg. The mitochondrial membrane potential was assessed using a JC-1 fluorescent probe, JC-1 is at the state of aggregates (red fluorescence); when the mitochondrial membrane potential is decreased, JC-1 can be de-aggregated into monomers (green fluorescence), indicating mitochondrial damage. Calculate the ratio of red to green fluorescence.

Detection of ROS and MDA levels in hypothalamic tissue using ELISA

Rat ROS and MDA levels in hypothalamic tissues were measured using double-antibody sandwich ELISA kits, following the manufacturer's instructions. Approximately 100 μg of fresh left hypothalamic tissue was collected, and 3 mL of PBS was added. The tissue was homogenized using a glass homogenizer and then centrifuged to obtain the supernatant. The sample was added to the bottom of the enzyme-labeled plate well and gently shaken to mix. After adding the enzyme and incubating, it was washed five times with a detergent, and then dried. The chromogenic agent was added, gently shaken to mix, and incubated at 37 °C in the dark for 15 min. The reaction was terminated with the termination solution, and the absorbance (OD value) was measured at a wavelength of 450 nm with an enzyme-labeled instrument. The content of reactive oxygen species (ROS) in the sample was calculated through the standard curve.

TUNEL staining

TUNEL staining was used to observe rat hypothalamic tissue apoptosis. Paraffin sections of the rat hypothalamus were dewaxed with an ethanol gradient, dehydrated, and sealed at room temperature for 1 h. Endogenous peroxidases were blocked with 3% H_2O_2 for 10 min and washed twice with PBS. TUNEL and DAPI staining was performed according to the TUNEL kit instructions. Apoptosis was observed using fluorescence microscopy (Nikon) with green and blue fluorescence indicating apoptotic cells and nuclei, respectively. Five Random visual fields from each microscopic section were analyzed, and the apoptosis index was calculated as the number of positive cells divided by the total number of cells multiplied by 100%.

Measurement of p-mTOR, mTOR, Pink1, Parkin, P62, and LC3 expression in rat hypothalamic tissues, and calculation of the LC3II/LC3I ratio

Fresh hypothalamus tissue (100 μg) was placed in a centrifuge tube containing 1 mL of RIPA lysate for grinding and centrifugation. After extracting the protein from the supernatant, its concentration was determined using a bicinchoninic acid kit. The protein sample was then subjected to electrophoresis and transferred to a membrane that was sealed with skim milk powder. Antibody working solutions were prepared according to the manufacturer's instructions (Pink1, Parkin, P62, and LC3 antibodies were diluted 1:2000, and p-mTOR and mTOR antibodies were diluted 1:1000). The primary antibody was incubated overnight on a shaker at 4 ℃, followed by incubation with the corresponding secondary antibody (1:5000) at room temperature for 1 h. Signal intensity was detected using an ECL chemiluminescence imaging system. The optical density of the bands was analyzed using ImagePro Plus 6.0, and the relative expression was calculated relative to the ratio of the absorbance of the target protein to that of GAPDH.

Immunofluorescence analysis

Paraffin sections of the rat hypothalamus were deparaffinized using a gradient of ethanol, dehydrated, dried, and washed three times with PBS. The sections were then sealed at room temperature with 1‰ Triton-X-100 and 2% sheep serum for 1 h. Following washing with PBS, the sections were incubated overnight at 4 ℃ with primary antibodies against Pink1 (1:150), Parkin (1:100), LC3 (1:100), and Tom20 (1:150). After washing to remove the primary antibody, sections were incubated at room temperature for 30 min with secondary antibodies: goat anti-rabbit fluorescence II (DyLight 594, 1:500) or goat anti-mouse fluorescence II (DyLight 488, 1:500). Following additional PBS washes, the nucleus was stained with DAPI. The co-localization of Pink1 with Parkin, LC3, and Tom20 in the hypothalamus was observed using confocal microscopy (Olympus FV3000).

Statistical analysis

Statistical analyses were performed using the GraphPad Prism 9 software. Data are expressed as mean ± SD. A one-way analysis of variance was used to compare multiple groups, followed by the SNK-q test for pairwise comparisons. Differences were considered statistically significant at $P < 0.05$.

Results

Changes in the core temperature of each group

As shown in Fig. 1, before modeling, the core temperatures of rats in all four groups were approximately 37 ℃, with no significant difference ($P > 0.05$). During the modeling process, the core temperatures in the CON and RAPA groups remained stable at around 37 ℃. In contrast, the core temperatures of the EHS and EHS + RAPA

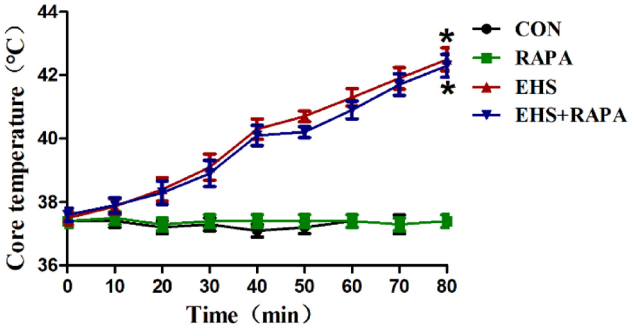

Fig. 1. Changes in core temperature in each group of rats. *$P < 0.05$ vs. control group; RAPA group($n = 10$): normal rats injected with rapamycin. EHS($n = 5$): Exertional heat stroke model group, EHS + RAPA group($n = 8$): Rapamycin-injected model group.

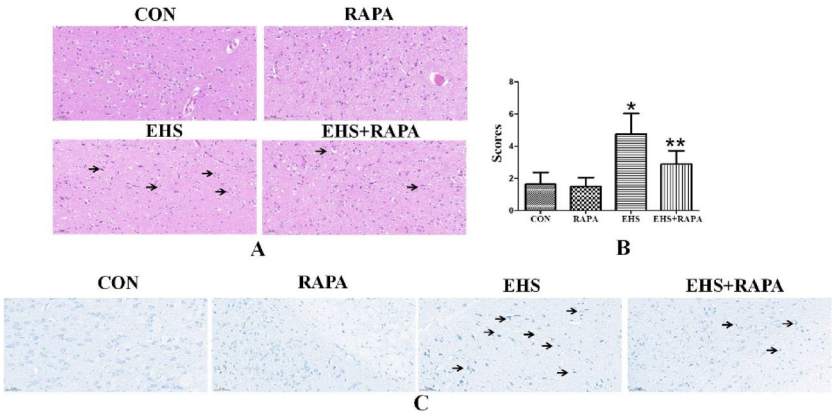

Fig. 2. Histological changes in the hypothalamus of rats in each group. (**A**) HE staining of the hypothalamus. (**B**) Pathological damage score of the hypothalamus in rats: *$P < 0.05$ vs. control group, *$P < 0.05$ vs. EHS group. (**C**) Hypothalamus Nissl staining. RAPA group($n = 10$): Normal rats injected with rapamycin, EHS($n = 5$): Exertional heat stroke model group, EHS + RAPA group($n = 8$): Rapamycin-injected model group. Bar: 50 μm.

groups increased sharply. After 80 min in the cabin, the core temperatures of these two groups exceeded 42 ℃, which was considerably higher than that of the CON group.

RAPA alleviates pathological injury in the hypothalamic tissue of rats with EHS

HE staining (Fig. 2A) revealed a clear hypothalamic structure with normal cell morphology and loose nuclear chromatin in the CON and RAPA groups. In the EHS group, numerous neurons exhibited nuclear pyknosis and deep staining (black arrow), with a reduction or absence of perinuclear cytoplasm. Compared to the EHS group, the EHS + RAPA group had fewer deeply stained neurons and a lower degree of nuclear pyknosis. The pathological score of the hypothalamus (Fig. 2B) was significantly higher in the EHS group than in the CON group ($P < 0.001$); in contrast, the score in the EHS + RAPA group was significantly lower than that in the EHS group ($P = 0.0014$). There were no significant differences between the CON and RAPA groups ($P > 0.05$). Nissl staining revealed a clear hypothalamic structure with uniformly distributed Nissl bodies in the CON group. In contrast, the EHS group exhibited a loss of Nissl bodies, along with pyknotic and hyperchromatic neuronal nuclei (black arrow). The EHS + RAPA group exhibited a clearer structure of Nissl bodies and reduced pyknosis and hyperchromatism of neuronal nuclei compared to the EHS group (Fig. 2C).

RAPA alleviates apoptosis in the hypothalamic tissue of rats with EHS

Compared to the CON group, the number of apoptotic cells and the apoptotic index in the hypothalamus were increased in the EHS group ($P < 0.0001$); in contrast, both were significantly decreased in the EHS + RAPA group ($P < 0.0001$). There was no significant difference in the hypothalamic apoptotic index between the CON and RAPA groups ($P = 0.99$) (Fig. 3).

RAPA decreases mitochondrial membrane potential and oxidative stress product levels in the hypothalamic tissue of rats with EHS

The JC-1 assay was used to determine the mitochondrial membrane potential (Fig. 4A). It was found that the mitochondrial membrane potential of hypothalamus was significantly lower in the EHS group than in the

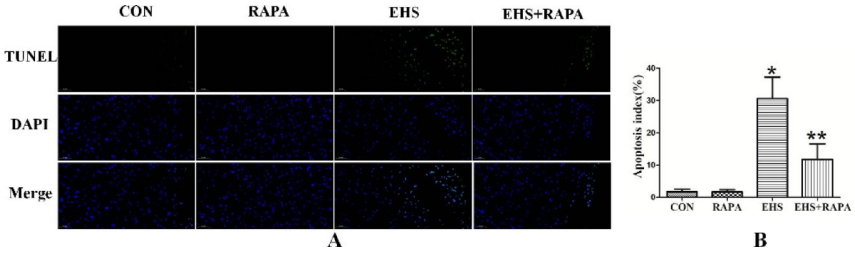

Fig. 3. Rapamycin reduced hypothalamic cell apoptosis in rats with EHS (**A**) TUNEL staining of rat hypothalamic tissues. (**B**) Pathological injury score of rat hypothalamus: *$P < 0.05$ vs. control group, *$P < 0.05$ vs. EHS group.

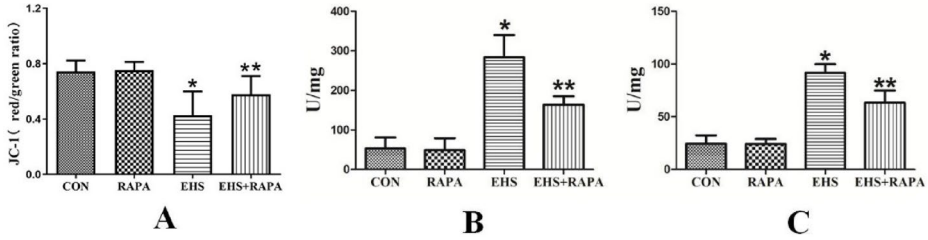

Fig. 4. Rapamycin affected MMP(JC-1), ROS, and MDA levels in the hypothalamus of rats with EHS (**A**) Changes in mitochondrial membrane potential (JC-1) in the rat hypothalamus. (**B**) Changes in ROS levels in the rat hypothalamus. (**C**) Changes in MDA levels in the rat hypothalamus. *$P < 0.05$ vs. control group, *$P < 0.05$ vs. EHS group.

CON group ($P < 0.0001$). The mitochondrial membrane potential of hypothalamus was significantly higher in the EHS + RAPA group than in the EHS group ($P = 0.0057$), while there was no significant difference in mitochondrial membrane potential between the CON and RAPA groups ($P > 0.99$). The results for oxidative stress products (Fig. 4B, C) indicated low ROS and MDA levels in the hypothalamus of the CON and RAPA groups, with no significant differences ($P > 0.05$). In contrast, ROS and MDA levels were significantly increased in the EHS group compared to the CON group ($P < 0.0001$); however, both levels were significantly lower in the EHS + RAPA group compared to the EHS group ($P < 0.0001$).

RAPA enhances mitochondrial autophagy in the hypothalamic tissue of rats with EHS

Western blotting results showed that (Fig. 5A, B), compared to the CON group, the ratio of the autophagy marker LC3-II/LC3-I in the hypothalamic tissues of rats with EHS was increased ($P < 0.05$), whereas p62 expression was decreased ($P = 0.0024$). In the EHS + RAPA group, the LC3-II/LC3-I ratio was further increased ($P = 0.0107$), and p62 expression was further decreased ($P = 0.0083$) compared to the EHS group, while no significant differences were observed in the LC3-II/LC3-I ratio or p62 expression between the CON and RAPA groups ($P > 0.99$).

To further verify the effect of RAPA on mitochondrial autophagy, hypothalamic immunofluorescence staining was performed. As shown in Fig. 5C, co-localization of the autophagy protein LC3 (red fluorescence) and mitochondrial protein Tom20 (green fluorescence) in hypothalamic neurons was weak in the CON and RAPA groups (no obvious orange fluorescence). Compared to the CON group, the co-localization (orange fluorescence) of LC3 and Tom20 in the cytoplasm of hypothalamic neurons was significantly enhanced in the EHS group. This co-localization was further enhanced in the EHS + RAPA group compared to the EHS group. (Fig.S1)

Effects of RAPA on the p-mTOR, mTOR, and Pink1/Parkin pathways in the hypothalamic tissue of rats with EHS

Western blotting showed that (Fig. 6A, B) the protein expression of p-mTOR, Pink1, and Parkin in the hypothalamus was higher in the EHS group than in the CON group ($P < 0.0001$). After RAPA administration, the p-mTOR protein expression in the hypothalamus was significantly decreased in the EHS + RAPA group ($P < 0.0001$), whereas that of Pink1 and Parkin was further increased ($P < 0.0001$). In contrast, there was no significant difference in the p-mTOR/mTOR ratio between the CON and RAPA groups. Although Pink1 and Parkin expression in the hypothalamus was higher in the RAPA group than in the CON group, the difference was not significant ($P = 0.0837$).

To further explore the effect of RAPA on the interaction between Pink1 and Parkin, immunofluorescence co-staining was performed on rat hypothalamic tissue (Fig. 6E). As shown in Fig. 6C, D, the co-localization of Pink1 (red fluorescence) and Parkin (green fluorescence) in the cytoplasm of hypothalamic neurons was weak in the CON group (no obvious orange fluorescence). The co-localization of Pink1 and Parkin was slightly

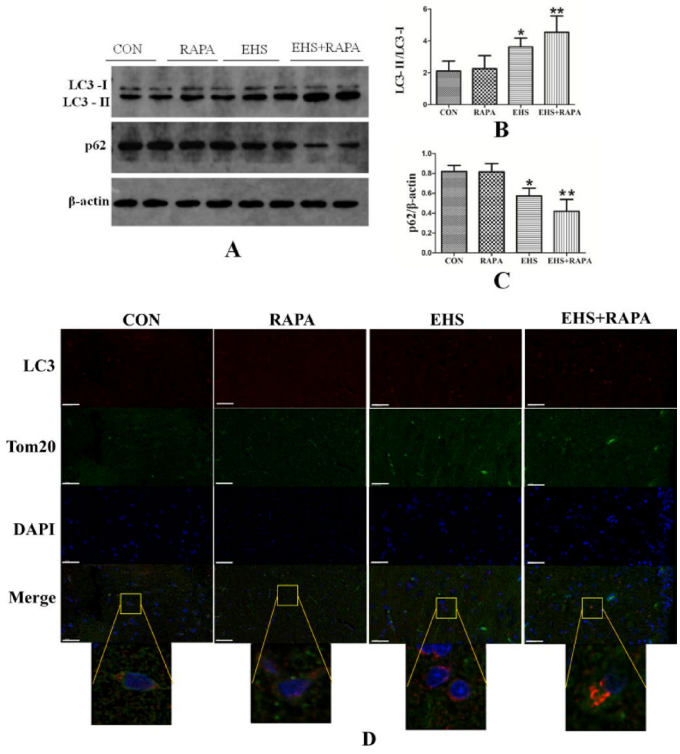

Fig. 5. Rapamycin upregulated mitophagy in the hypothalamus of rats with EHS. **A**. Western blot results for LC3 and p62 in rat hypothalamus. **B** and **C**. Statistical analysis of the LC3-Ⅱ/LC3-Ⅰ ratio and p62 protein expression in the rat hypothalamus. *$P < 0.05$ vs. control group, *$P < 0.05$ vs. EHS group. D. Immunofluorescence co-staining of LC3 and Tom20 in hypothalamic neurons. Bar: 20 μm. RAPA group($n = 10$): Normal rats injected with rapamycin, EHS($n = 5$): Exertional heat stroke model group, EHS + RAPA group($n = 8$): Rapamycin-injected model group.

stronger in the RAPA group than in the CON group. In the EHS group, the co-localization of Pink1 and Parkin in the cytoplasm of hypothalamic neurons was significantly enhanced compared to the CON group. This co-localization was further enhanced in the EHS + RAPA group compared to the EHS group. (Fig.S2)

Discussion

This study successfully established a rat model of EHS, a fatal condition caused by heat injury and strenuous exercise. EHS is characterized by a sharp rise in core temperature and severe central nervous system dysfunction[16]. It was observed that the core temperature of rats with EHS rapidly increased to 42 °C, resulting in pathological hypothalamic tissue damage and increased hypothalamic neuronal apoptosis, confirming central nervous system injury in these rats. These findings are consistent with those of previous studies[17,18].

The mechanism underlying organ function damage caused by EHS remains unclear. Studies suggest that abnormal oxidative stress levels, driven by ROS production and an imbalance in antioxidant enzyme activity, could be key mechanisms underlying central nervous system injury[19,20]. Oxidative stress caused by the accumulation of oxygen-free radicals is the core event of secondary damage following EHS. Oxidation stress intensifies injury caused by hyperthermia and physical exhaustion[21]. The study also found that the levels of oxidative stress products ROS and MDA were significantly elevated in the hypothalamus of rats exposed to heat stress, indicating that EHS triggers a strong oxidative stress response in the hypothalamus. A high ROS level induces apoptosis and necrosis of neurons, resulting in central nervous system dysfunction.

Increasing evidence suggests that the body selectively removes damaged or dysfunctional mitochondria through mitochondrial autophagy to maintain mitochondrial quality and homeostasis. Alterations in mitochondrial autophagy are linked to various diseases, including neurodegenerative disorders, heart failure, cancer, and aging[22–24]. The Pink1/Parkin pathway is a classical mitochondrial autophagy pathway activated under cellular stress[25,26]; it is involved in mitochondrial metabolism and redox homeostasis[27]. ROS produced by mitochondria directly induce mitochondrial autophagy[28]. In contrast, Pink1/Parkin-dependent mitochondrial autophagy requires the production of O_2^-. Therefore, oxidative stress triggers Pink1/Parkin-dependent mitochondrial autophagy.

Our results showed that in the hypothalamus of rats subjected to EHS, the mitochondrial membrane potential decreased, oxidative stress products (ROS and MDA) increased, and the expression of Pink1 and Parkin increased. The interaction between these proteins was enhanced, leading to increased mitochondrial

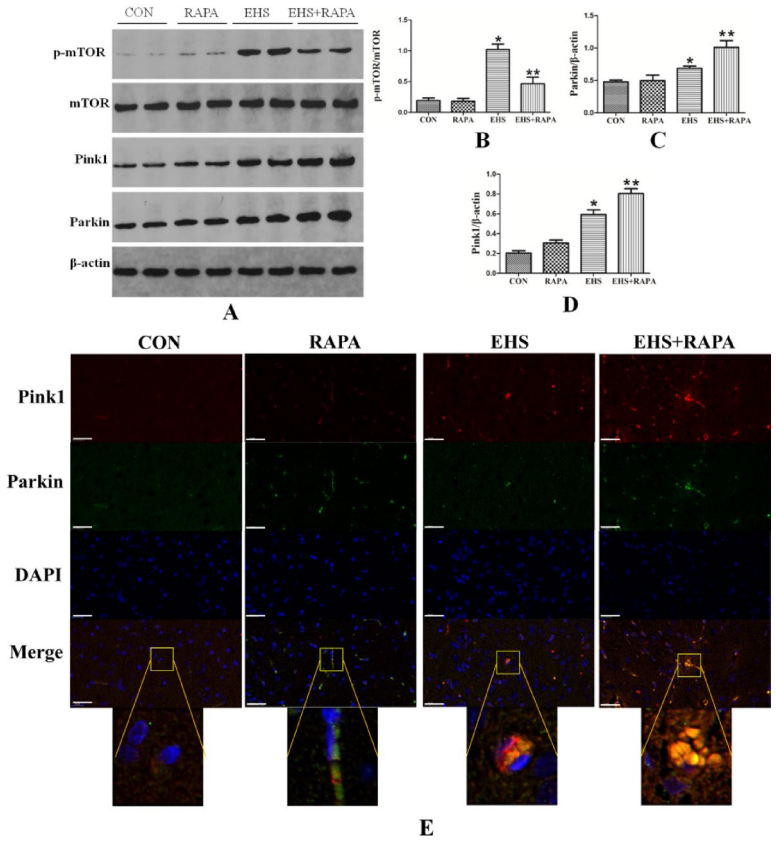

Fig. 6. Rapamycin inhibited mTOR and activated the Pink1/Parkin pathway in the hypothalamus of rats with EHS. **A**. Western blot results for p-mTOR, mTOR, Pink1, and Parkin in the rat hypothalamus. **B**–**D**. Statistical analysis of the p-mTOR/mTOR ratio and Pink1 and Parkin protein expression in the rat hypothalamus. $^{*}P < 0.05$ vs. control group, $^{*}P < 0.05$ vs. EHS group. E. Immunofluorescence co-staining of Pink1 and Parkin in the rat hypothalamus. Bar: 20 μm. RAPA group($n = 10$): Normal rats injected with rapamycin, EHS($n = 5$): Exertional heat stroke model group, EHS + RAPA group($n = 8$): Rapamycin-injected model group.

autophagy. These findings confirm that EHS causes mitochondrial damage in the hypothalamus and enhances oxidative stress, activating Pink1/Parkin-dependent mitochondrial autophagy.

In the normal state of mitochondria, the N-terminal of PINK 1 is constitutively transported into the mitochondrial inner membrane through translation. The MTS of PINK 1 on the mitochondrial inner membrane is cut off, and the PINK 1 from the removed MTS is released into the cytoplasm and then degraded by the proteasome. When mitochondria are damaged and depolarized, the N-terminal of PINK 1 cannot be translocated to the mitochondrial inner membrane, resulting in the accumulation of PINK 1 on the mitochondrial outer membrane[29]. PINK 1 further activates the E3 ubiquitin Ligase activity of Parkin by phosphorylating the Ser 65 residue in Ub1[30]. The OMM protein attached to the mitochondrial outer membrane is ubiquitinated by the E3 ligase Parkin. The ubiquitinated OMM protein is recognized by p62 as a recognition substance and then targets protein aggregates for autophagosome formation through the LC 3 interaction domain (LIR) motif[31].

Therefore, the Pink1/Parkin signaling pathway may serve as a target for treating EHS-induced diseases. Pink1/Parkin pathway activation and increased mitochondrial autophagy mitigate hypothalamic injury caused by EHS.

RAPA was selected as an inducer of mitochondrial autophagy. The results demonstrated that RAPA reduced hypothalamic pathological damage and apoptosis, decreased oxidative stress in the hypothalamus, and maintained mitochondrial membrane potential stability in EHS-fed rats. Another study found that RAPA inhibited mTOR phosphorylation in the hypothalamus of rats with EHS, increased Pink1 and Parkin protein levels (Fig. 6A), enhanced Pink1 and Parkin binding (Fig, 6E), and upregulated mitochondrial autophagy levels (Fig. 5A–D).

Therefore, although EHS can induce a compensatory increase in Pink1/Parkin-mediated mitochondrial autophagy in the hypothalamus, it is insufficient to clear damaged mitochondria and maintain mitochondrial dynamic stability. RAPA reduces hypothalamic neuronal damage and preserves hypothalamic function by inhibiting mTOR and activating Pink1/Parkin-dependent mitochondrial autophagy.

In conclusion, we demonstrated that mitochondrial damage and increased oxidative stress are mechanisms of hypothalamic injury caused by EHS. Our results also show that RAPA mitigates EHS-induced hypothalamic injury by inhibiting mTOR and activating the Pink1/Parkin pathway, thereby enhancing mitochondrial autophagy.

Limitations of this study

Two aspects of our study require some caution when interpreting the results. First, we have to admit the implications of the smaller sample size on the interpretation of our results and the potential limitations it introduces in terms of generalizability. We have conducted post-hoc power analyses to quantify the impact of this discrepancy on our findings. Second, in this experiment, we focused on specific end-points that align with our hypothesis and the experimental design aimed at assessing the immediate effects of RAPA on mitophagy. However, time-course data could provide deeper insights into the dynamics of the response, in the next stage of our research, we will dynamically detect the mitochondrial autophagy induced by RAPA.

Data availability

The data that support the findings of this study are available from the corresponding author upon reasonable request.

Received: 27 December 2024; Accepted: 15 September 2025
Published online: 23 October 2025

References

1. Liu, S. Y., Song, J. C., Mao, H. D., Zhao, J. B. & Song, Q. Expert consensus on diagnosis and treatment of heat stroke in China. *Mil Med. Res.* **7**, 1 (2020).
2. Yan, R., Yang, M. M., Zhang, Y., Liu, S. F. & Kang, H. J. Research advances in prevention of central nervous system injury of heat stroke. *Acad. J. Chin. PLA Med. Sch.* **39**, 1004–1007 (2018).
3. Xv, F. et al. Quantitative proteomics provided insights into the protective effects of heat acclimation on the rat hypothalamus after exertional heatstroke. *J. Integr. Neurosci.* **23**, 116 (2024).
4. Algothmi, K. M. et al. Protective impacts of mitochondria enhancers against thermal stress in poultry. *Poult. Sci.* **103**, 103218 (2024).
5. Zhang, Z. et al. Heat stroke: Pathogenesis, diagnosis, and current treatment. *Ageing Res. Rev.* **100**, 102409 (2024).
6. Iba, T., Helms, J., Levi, M. & Levy, J. H. Inflammation, coagulation, and cellular injury in heat-induced shock. *Inflamm. Res.* **72**, 463–473 (2023).
7. Wang, L. et al. Selective oxidative stress induces dual damage to telomeres and mitochondria in human T cells. *Aging Cell.* **20**, e13513 (2021).
8. Kumar, R. & Reichert, A. S. Common principles and specific mechanisms of mitophagy from yeast to humans. *Int. J. Mol. Sci.* **22**, 4363 (2021).
9. Beesetti, S. et al. FANCL supports Parkin-mediated mitophagy in a ubiquitin ligase-independent manner. *Biochim. Biophys. Acta Mol. Basis Dis.* **1868**, 166453 (2022).
10. Huang, W. et al. Cytosolic p53 inhibits Parkin-mediated mitophagy and promotes acute liver injury induced by heat stroke. *Front. Immunol.* **13**, 859231 (2022).
11. Zou, C. Y., Chen, C., Wang, F. Q., Ruan, H. J. & Lyu, J. Research progress of autophagy modulators targeting PI3K/Akt/mTOR signaling pathway. *Chin. J. Med. Chem.* **31**, 825–833 (2021).
12. Tao, D. et al. Rapamycin mitigates neurotoxicity of fluoride and aluminum by activating autophagy through the AMPK/mTOR/ULK1 pathway in hippocampal neurons and NG108-15 cells. *Sci. Rep.* **15**, 9801 (2025).
13. He, S. X. et al. Optimization of a rhabdomyolysis model in mice with exertional heat stroke mouse model of EHS-Rhabdomyolysis. *Front. Physiol.* **11**, 642 (2020).
14. Mao, H. D. et al. Application of implantable biotelemetry in rat model of exertional heat stroke. *Acad. J. Chin. PLA Med. Sch.* **42** (1doi), 1068–1073 (2021).
15. Thoresen, M. et al. A piglet survival model of posthypoxic encephalopathy. *Pediatr. Res.* **40**, 738–748 (1996).
16. Epstein, Y. et al. Exertional heat illness: international military-oriented lessons learned and best practices for prevention and management. *Front. Physiol.* **16**, 1456984 (2025).
17. Zaretsky, D. V. et al. Disinhibiting neurons in the dorsomedial hypothalamus delays the onset of exertional fatigue and exhaustion in rats exercising in a warm environment. *Brain Res.* **1689**, 12–20 (2018).
18. Li, J. et al. Heat acclimation defense against exertional heat stroke by improving the function of preoptic TRPV1 neurons. *Theranostics* **15**, 1376–1398 (2025).
19. Dokladny, K., Myers, O. B. & Moseley, P. L. Heat shock response and autophagy–cooperation and control. *Autophagy* **11**, 200–213 (2015).
20. Ran, L. Y. et al. Integrated transcriptomic and proteomic analysis indicated that neurotoxicity of rats with chronic fluorosis May be in mechanism involved in the changed cholinergic pathway and oxidative stress. *J. Trace Elem. Med. Biol.* **64**, 126688 (2021).
21. Hsu, S. F., Niu, K. C., Lin, C. L. & Lin, M. T. Brain cooling causes Attenuation of cerebral oxidative stress, systemic inflammation, activated coagulation, and tissue ischemia/injury during heatstroke. *Shock* **26**, 210–220 (2006).
22. Wang, L., Lu, G. & Shen, H. M. The long and the short of PTEN in the regulation of mitophagy. *Front. Cell. Dev. Biol.* **8**, 299 (2020).
23. Moyzis, A. G., Sadoshima, J. & Gustafsson, Å. Mending a broken heart: the role of mitophagy in cardioprotection. *Am. J. Physiol. Heart Circ. Physiol.* **308**, H183–192 (2015).
24. Chen, G., Kroemer, G. & Kepp, O. Mitophagy: an emerging role in aging and Age-Associated diseases. *Front. Cell. Dev. Biol.* **8**, 200 (2020).
25. Bader, V. & Winklhofer, K. F. PINK1 and parkin: team players in stress-induced mitophagy. *Biol. Chem.* **401**, 891–899 (2020).
26. Zhang, S. M., Fan, B., Li, Y. L., Zuo, Z. Y. & Li, G. Y. Oxidative stress-involved mitophagy of retinal pigment epithelium and retinal degenerative diseases. *Cell. Mol. Neurobiol.* **43**, 3265–3276 (2023).
27. Wang, Y., Nartiss, Y., Steipe, B., McQuibban, G. A. & Kim, P. K. ROS-induced mitochondrial depolarization initiates PARK2/Parkin-dependent mitochondrial degradation by autophagy. *Autophagy* **8**, 1462–1476 (2012).
28. Lu, Y. et al. Cellular mitophagy: mechanism, roles in diseases and small molecule Pharmacological regulation. *Theranostics* **13**, 736–766 (2023).
29. Furukawa, K., Innokentev, A. & Kanki, T. Regulatory mechanisms of mitochondrial autophagy: lessons from yeast. *Front. Plant. Sci.* **10**, 1479 (2019).
30. Chu, C. T. Mechanisms of selective autophagy and mitophagy: implications for neurodegenerative diseases. *Neurobiol. Dis.* **122**, 23–34 (2019).
31. Zhou, T. Y. et al. Review of PINK1-Parkin-mediated mitochondrial autophagy in alzheimer's disease. *Eur. J. Pharmacol.* **959**, 176057 (2023).

Acknowledgements
We thank Master Liya Jiang and Master Yunya Ma for their selfless help in model preparation and specimen collection and Hanzhi Mao for his selfless help in histopathological analysis.

Author contributions
Guarantor of integrity of the entire study: Ruxue Chi, Jiaxing Wang, Yuxiang Zhang Study concepts: Ruxue Chi, Ran Meng, Lv Xuan Study design: Ruxue Chi, Jiaxing Wang, Ran Meng, Yan Gu, Yuxiang Zhang Definition of intellectual content: Ruxue Chi, Jiaxing Wang, Ran Meng, Lv Xuan, Yan Gu, Yuxiang Zhang Experimental studies: Ruxue Chi, Jiaxing Wang, Ran Meng, Lv Xuan, Yuxiang Zhang, Zhengzhong Sun Statistical analysis: Ruxue Chi, Ran Meng, Yan Gu Manuscript preparation: Ruxue Chi, Ran Meng Manuscript editing: Ruxue Chi, Ran Meng Manuscript review: Jiaxing Wang, Yuxiang Zhang All authors have read and approved this article.

Funding
This study was supported by the 2020 Military Health and Epidemic Prevention Special Task (Guard Letter [2020] No. 208), 2023 Military Health and Epidemic Prevention Special Task (Guard Letter [2023] No. 365), and the School Project (2016ZD-008).

Competing interests
The authors declare no competing interests.

Ethical statement
All animal experiments are in in accordance with ARRIVE guidelines.

Additional information
Supplementary Information The online version contains supplementary material available at https://doi.org/10.1038/s41598-025-20313-1.

Correspondence and requests for materials should be addressed to Y.G., Y.Z. or J.W.